

Nonstatistical Ratios of Photoionization Cross Sections for States Split by Spin-Orbit Coupling*

T. E. H. Walker, J. Berkowitz, and J. L. Dehmer
Argonne National Laboratory, Argonne, Illinois 60439

and

J. T. Waber
Department of Materials Science, Northwestern University, Evanston, Illinois 60201
 (Received 5 July 1973)

From photoelectron spectroscopic studies at 584 Å, the ${}^2D_{5/2} : {}^2D_{3/2}$ intensity ratios of Zn, Cd, and Hg have been determined, and the latter two were found to be significantly larger than the statistical value $(l+1)/l$. Earlier experiments on Ar, Kr, and Xe have yielded ${}^2P_{3/2} : {}^2P_{1/2}$ ratios smaller than statistical. We present Dirac-Slater calculations of the partial photoionization cross sections for the $j = l \pm \frac{1}{2}$ components of an atomic orbital which show that the ratio is larger or smaller than the statistical value depending on whether the partial cross sections are rising or falling.

It has been apparent for some time that spin-orbit coupling can affect the details of photoionization and photoelectron spectra.¹ In particular, the photoionization cross sections for the two spin-orbit components of a given orbital are not always in the ratio predicted by the two occupation numbers.²⁻⁴ A number of investigators⁴ have reported the ${}^2P_{3/2} : {}^2P_{1/2}$ ratios for Ar, Kr, and Xe to be less than the statistical value of 2:1 at 584 Å. Conversely, we have found the ${}^2D_{5/2} : {}^2D_{3/2}$ ratios for Cd and Hg are greater than their statistical ratio of 3:2 at this wavelength. With this in mind, we have performed Dirac-Slater⁵ calculations to obtain theoretical cross sections at low photon energies. The full details of these calculations will be dealt with in a forthcoming paper, and only a brief outline is given here.

Self-consistent calculations were carried out for the ${}^2D_{3/2}$ and ${}^2D_{5/2}$ states of Zn⁺, Cd⁺, and Hg⁺ corresponding to removal of the least tightly bound *d* orbital, and the potentials thus obtained were used as input for the continuum orbital program. To maintain orthogonality, the ion wave functions were also used to describe the bound *d* orbitals. The value⁶ of the parameter α , which determines the exchange contribution in the Slater approximation, was taken to be $\frac{2}{3}$, in keeping with previous Dirac-Slater calculations.⁵ Matrix elements were calculated both in the lowest dipole approximation, and by including matrix elements of $j_0(\omega r)$ and $j_2(\omega r)$, where ω is the photon momentum, and j_0, j_2 are spherical Bessel functions. Inclusion of these Bessel functions made virtually no difference in the values of the matrix elements. From the calculated matrix elements and the experimental ionization potentials, the

partial photoionization cross sections for removal of the $d_{3/2}$ and $d_{5/2}$ electrons can be calculated. This is shown for mercury in Fig. 1, where we have displayed the cross section *per electron*. For all these atoms, the $d_{5/2}$ partial cross section per $d_{5/2}$ electron is larger at threshold than that of the $d_{3/2}$, has a slightly larger maximum, and begins to decrease first. After the maximum, the cross section per $d_{3/2}$ electron is larger than that of the $d_{5/2}$. The observed intensity ratio for the two ionizations will be given by the product of the ratio of cross sections per electron and the ratio of the number of electrons in each orbital. Thus, if the partial cross sections per electrons are the same, the ratio $\sigma_{5/2}/\sigma_{3/2}$ would equal 3:2, where σ_n is the partial cross section for photoionization from the *n*th orbital.

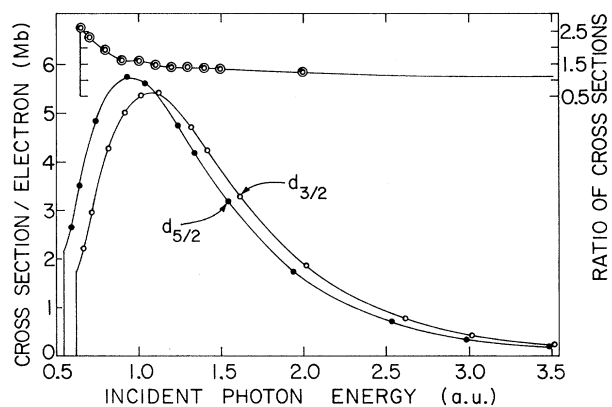


FIG. 1. Cross section per electron for photoionization of the $5d_{5/2}$ and $5d_{3/2}$ of mercury as a function of incident photon energy. The topmost curve shows $\sigma_{5/2}/\sigma_{3/2}$ as a function of incident photon energy.

TABLE I. Ratios of photoionization cross sections ($\sigma_{5/2}/\sigma_{3/2}$) at 21.2 eV.

Atom	Orbital	Calc.	Obs.
Zn	3d	1.582	1.50
Cd	4d	1.746	1.79
Hg	5d	2.025	2.18, 2.38 ^a

^aD. C. Frost, C. A. McDowell, and D. A. Vroom, Chem. Phys. Lett. 1, 93 (1967).

These calculations are compared at 584 Å with our measurements on Zn, Cd, and Hg in Table I. The experiments were performed with a cylindrical-mirror photoelectron spectrometer and oven system described elsewhere.⁷ The agreement between experiment and theory in Table I is good.

Our calculations have been extended to higher energies, and Fig. 2 shows the photoionization cross section per electron of the 5d orbital of mercury around the Cooper minimum.¹ The minimum occurs first in $\sigma_{5/2}$; once the cross section per $d_{5/2}$ electron begins to rise, it becomes larger than that of the $d_{3/2}$. At still higher energies, when the 5d cross section begins to fall, the cross section per $d_{3/2}$ electron is again larger than that of the $d_{5/2}$.

A comparison of the matrix elements into the p and f partial waves shows that these effects are dominated by the $d \rightarrow f$ channel. This is to be expected because the $l+1$ channel usually dominates the cross section.⁸ It is therefore possible to discuss these results qualitatively by ignoring the $l-1$ channel, and using the model^{1,8} previously introduced to explain the Cooper minimum.

At very low photoelectron energies the first major maximum of the continuum orbital of the $l+1$ channel will lie outside the region of space occupied by the bound orbital. As the photoelectron energy increases, this maximum moves nearer the nucleus, and the dipole matrix element increases. As the photoelectron energy increases still further, the first major maximum of the continuum orbital begins to overlap the nodes of the bound orbital (if any) and the dipole matrix element decreases and finally changes sign, giving rise to the Cooper minimum in the partial cross section.

Now consider what happens when spin-orbit coupling is introduced. This results in the $j = l - \frac{1}{2}$ component of the bound orbital, for which the spin-orbit interaction is attractive, being slightly closer to the nucleus than the $j = l + \frac{1}{2}$. As a result, when the photoelectron energy in-

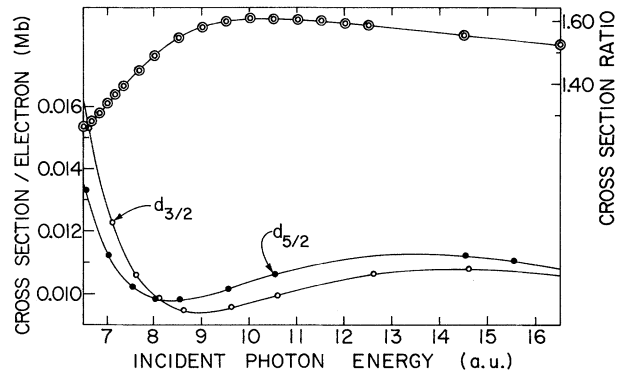


FIG. 2. Cross section per electron for photoionization of the $5d_{5/2}$ and $5d_{3/2}$ of mercury as a function of incident photon energy. The topmost curve shows $\sigma_{5/2}/\sigma_{3/2}$ as a function of incident photon energy.

creases from zero, the continuum orbital will have a greater overlap with the $j = l + \frac{1}{2}$ component of the bound state, and the ratio $\sigma_{l+1/2}/\sigma_{l-1/2}$ will be greater than the statistical value of $(l+1)/l$. Figure 3 illustrates this. Similarly, the continuum orbital will overlap the outermost node of the $j = l + \frac{1}{2}$ before that of the $j = l - \frac{1}{2}$, and in this part of the spectrum, where the cross section is decreasing, $\sigma_{l+1/2}/\sigma_{l-1/2} < (l+1)/l$. The same pattern repeats after the Cooper minimum has been passed. Thus we can make the generalization that if the partial cross section is rising, the ratio of cross sections is greater than statistical, while if the partial cross section is falling, the ratio will be less than statistical.

Both situations may now be corroborated with experimental data. At 584 Å the partial cross sections for Zn,⁹ Cd,¹⁰ and Hg¹¹ are rising.

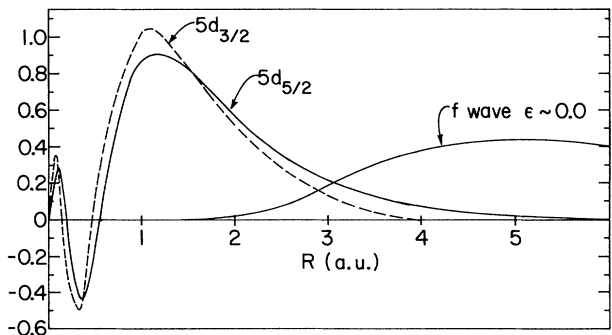


FIG. 3. Comparison of overlap of radial wave functions for $5d_{5/2}$ and $5d_{3/2}$ of mercury with f continuum wave ($\epsilon \sim 0$). The $5d_{5/2}$ wave function is drawn as calculated, but the $5d_{3/2}$ wave function is drawn to exaggerate the difference between the bound states, for clarity.

Hence, except for Zn, for which the spin-orbit effect is very small, the ${}^2D_{5/2}:{}^2D_{3/2}$ ratios are significantly larger than their statistical value. The analogous 2P ratios for Ar, Kr, and Xe are examples of smaller-than-statistical values since, in these cases, the cross section¹² is falling at 584 Å. It may be significant that for neon,⁴ where the measurement was made 0–2 eV above the ionization threshold and the cross section is still rising, the ratio was found to be 2.18.

Although a consideration of the difference in ground states is sufficient for a qualitative understanding of these results, there are other effects that can be important. Firstly, for a fixed photon energy, the photoelectron energy will be different for the two ionizations. This works in the same direction as the difference in ground-state wave functions. If the cross section is increasing with increasing photoelectron kinetic energy, the partial cross section of the channel with lower ionization potential, that is the $j = l + \frac{1}{2}$, will be favored; the reverse is true if the cross section is decreasing.

The relative importance of the kinetic-energy effect and the difference in wave functions of the two bound orbitals in determining the cross-section ratio varies with energy. At lower photon energies, when the photoelectron's kinetic energy is not very large compared to the spin-orbit splitting, the cross section is changing rapidly and the relative importance of the kinetic-energy effect will be at its largest. At these energies the kinetic-energy effect and the initial-state effect are roughly comparable. The kinetic-energy effect alone was evaluated for Hg at 584 Å in a nonrelativistic calculation¹³ which yielded a ratio of 1.79. The initial-state effect can be estimated from our calculation by comparing cross sections corresponding to equal photoelectron energies. This yields ratios of 1.71 and 1.65 for kinetic energies of 0.2 and 0.3 a.u., respectively. As the photoelectron energy becomes much larger than the spin-orbit splitting, its influence diminishes and the nonstatistical behavior of the ratio will be predominantly an initial-state effect.

There will also be effects due to spin-orbit coupling in the continuum orbitals. We have found these to be small except near the Cooper minimum, and they are unlikely to affect the intensity ratio.

At very high energies, the continuum orbital exhibits rapid oscillatory behavior, and the dipole matrix elements are determined by the part of the wave function near the nucleus. Since the

$j = l - \frac{1}{2}$ component of the bound orbital is the more tightly bound, it would be expected to have the larger cross section per electron. This behavior is exhibited by our calculations at kinetic energies of 40 and 100 a.u., which yield ratios of 1.459 and 1.459 for Zn, 1.437 and 1.364 for Cd, and 1.416 and 1.340 for Hg. It is worth emphasizing that this behavior prevails even in the limit of high energy, so that the statistical ratio is not attained even as a limiting value.

The interpretation described in this Letter applies directly to closed-shell atoms, but is also applicable to other cases, such as deep inner shells, so long as the spin-orbit splitting is much larger than the coupling to the open shells. Otherwise the exact form of the angular momentum coupling will become important.¹⁴ In this short note, we may make some predictions for the $n\bar{p}$ electrons of the alkaline earths and the $4f$ of ytterbium. For the $2\bar{p}$ of magnesium the cross section rises from threshold,¹⁵ as it does for the $2\bar{p}$ of neon.¹ For the heavier alkaline earth metals, the partial cross section for ionization of the outer p orbital decreases from threshold,¹⁵ as it does for these orbitals of the corresponding rare gases. We have already seen that Ar, Kr, and Xe exhibit ${}^2P_{3/2}:{}^2P_{1/2}$ ratios less than statistical at 21.2 eV, whereas the one measurement reported for Ne is greater than statistical. We would predict a similar behavior for the alkaline earth metals a few volts beyond their respective p thresholds, the magnesium displaying a ${}^2P_{3/2}:{}^2P_{1/2}$ ratio greater than 2, and Ca, Sr, and Ba less than 2.

The case of Yb is somewhat more involved near threshold, because ionization of the f orbital is suppressed by a larger centrifugal barrier than the p and d previously considered. Hence, the $l + 1$ wave does not become significant for at least 0.5 a.u. beyond threshold.¹³ Between ca. 0.5 to 4 a.u. above threshold, the cross section into the $l + 1$ wave is increasing,¹⁵ and hence we would expect a ratio greater than 4:3.

It should be noted that the ratio of cross sections for the $5\bar{p}$ of xenon and the $3\bar{p}$ of argon have been correlated with the behavior of the Rydberg states in the work of Lu and co-workers^{3,16} using multichannel quantum defect theory. This approach is capable of giving much more detailed understanding and is necessary when channel interaction is strong. However, it does not lend itself readily to generalizations to all atoms.

One of us (T.E.H.W.) wishes to thank the Commonwealth Fund of New York for a Harkness

Fellowship. We are indebted to Dr. Y.-K. Kim for helpful conversations and his critical reading of the manuscript, and to Dr. S. T. Manson for communicating his unpublished results.

*Work performed under the auspices of the U.S. Atomic Energy Commission.

¹U. Fano and J. W. Cooper, *Rev. Mod. Phys.* **40**, 441 (1968).

²F. J. Comes and H. G. Sälzer, *Z. Naturforsch.* **19a**, 1230 (1964).

³K. T. Lu, *Phys. Rev. A* **4**, 579 (1971).

⁴J. A. R. Samson and R. B. Cairns, *Phys. Rev.* **173**, 80 (1968).

⁵D. Liberman, J. T. Waber, and D. T. Cromer, *Phys. Rev.* **137**, 27 (1965).

⁶J. C. Slater, *Advan. Quant. Chem.* **6**, 1 (1972).

⁷J. Berkowitz, *J. Chem. Phys.* **56**, 2766 (1972).

⁸J. W. Cooper, *Phys. Rev.* **128**, 681 (1962).

⁹H. Harrison, R. I. Schoen, R. B. Cairns, and K. E. Schubert, *J. Chem. Phys.* **50**, 3930 (1969).

¹⁰R. B. Cairns, H. Harrison, and R. I. Schoen, *J. Chem. Phys.* **51**, 5440 (1969).

¹¹R. B. Cairns, H. Harrison, and R. I. Schoen, *J. Chem. Phys.* **53**, 96 (1970).

¹²J. A. R. Samson, *Advan. At. Mol. Phys.* **2**, 177 (1966), and references therein.

¹³J. L. Dehmer, J. Berkowitz, and Y.-K. Kim, Proceedings of the Eighth International Conference on the Physics of Electronic and Atomic Collisions, Belgrade, Yugoslavia, 16-20 July 1973, Abstracts of Papers (to be published).

¹⁴A. R. P. Rau and U. Fano, *Phys. Rev. A* **4**, 1751 (1971).

¹⁵S. T. Manson, private communication.

¹⁶K. T. Lu and U. Fano, *Phys. Rev. A* **2**, 81 (1970);

C. M. Lee and K. T. Lu, *Phys. Rev. A* (to be published).

Thomas-Fermi Theory Revisited

Elliott H. Lieb*

Institut des Hautes Etudes Scientifiques, 91440-Bures-sur-Yvette, France

and

Barry Simon†

Department of Physics, Eidgenössische Technische Hochschule, CH-8049 Zurich, Switzerland

(Received 8 June 1973)

We show that the Thomas-Fermi theory is exact for atoms, molecules, and solids as $Z \rightarrow \infty$.

The Thomas-Fermi (TF) theory of atoms and molecules¹ is now more than 45 years old. The literature on the subject is vast² yet there remain more than a few unresolved problems both of principle and interpretation. Can one show that there is an electron density function ρ which actually minimizes the TF energy expression and that it satisfies the TF equation? Does this ρ represent the true electron density as computed from the Schrödinger equation as $Z \rightarrow \infty$? If so, there appear to be some "paradoxes": For atoms the density falls off exponentially with distance, while in TF theory³ it falls off as r^{-6} ; in TF theory atoms shrink in size as $Z^{-1/3}$ instead of growing; the electron density in TF theory is infinite at the nuclei instead of being finite; in TF theory molecules never bind.⁴

Recently, considerable progress has been made in showing that TF theory is applicable to high-

density matter,⁵ but the questions raised above are of a different nature, especially in the fact that a parameter in the problem, Z , becomes infinite; it is that which causes the electron density to become infinite. We report here the results of our analysis⁶ of the above questions, and the main conclusion is that TF theory, when correctly interpreted, is rigorously exact as $Z \rightarrow \infty$. We also show that TF theory is rigorously exact for solids in this limit and leads to a periodic ρ which satisfies the TF equation with the *periodic* Coulomb potential. This $Z \rightarrow \infty$ limit is related to, but is not the same as, the high-density limit with fixed Z , a case to which TF theory is often applied.⁷ We make no statements about this latter situation.

The TF energy functional in the presence of k nuclei of positive charges and positions (z_i, R_i) , $i = 1, \dots, k$, in units such that $\hbar^2(3/8\pi)^{2/3}(2m)^{-1} = 1$ and $|e| = 1$, is

$$E(\rho; z_1, \dots, z_k; R_1, \dots, R_k) = \frac{2}{5} \int \rho(x)^{5/3} d^3x + \frac{1}{2} \iint \rho(x)\rho(y) |x-y|^{-1} d^3x d^3y - \int \rho(x) \sum_{i=1}^k z_i |x-R_i|^{-1} d^3x. \quad (1)$$